Ind. J. Pharm. Edu. Res., 2026; 60(2s):s826-s838.
https://www.ijper.org

Original Article

Optimization of Ganciclovir-Loaded Nanoparticles for Ocular Delivery by Utilizing Box-Behnken Design

Shalu Verma[1], Divya Juyal[2,*]

[1]Department of Pharmaceutics, School of Pharmaceutical Sciences, Shri Guru Ram Rai University, Patel Nagar Campus, Patel Nagar, Dehradun, Uttarakhand-248001, INDIA.
[2]Department of Pharmacognosy, School of Pharmaceutical Sciences, Shri Guru Ram Rai University, Patel Nagar Campus, Patel Nagar, Dehradun, Uttarakhand-248001, INDIA.

ABSTRACT

Aim: The study aimed to optimize Ganciclovir-loaded nanoparticles for ocular delivery by evaluating the relationship between experimental data and Design factors. **Materials and Methods:** The nanoparticles were developed using the ionic gelation method. A 3-level, 3-factor Box-Behnken Design (BBD) was used for the optimisation process. Selecting the concentrations of chitosan, Sodium Tripolyphosphate (STPP) and sonication time as the independent variables. Entrapment efficiency, Drug release and Drug loading were chosen as dependent variables. The dependent and independent variables were related using response surface plots and the obtained polynomial equations. **Results:** The entrapment efficiency, Cumulative drug release and drug loading of the optimised Ganciclovir-loaded Chitosan Nanoparticles (GCV-CS-NPs) were found to be 91.93%, 92.27% and 17.68%, respectively. Excellent correlation between the dependent and independent response variables demonstrated the rationality of the optimised GCV-CS-NPS. **Conclusion:** The GCV release from GCV-CS-NPS exhibited a biphasic pattern, with a 2-hr rapid release after a 12-hr sustained release. Following the Peppas model, the *in vitro* release of the resulting ganciclovir-loaded nanoparticles demonstrated sustained release.

Keywords: Nanoparticles, Box-Behnken design, Ganciclovir, Ocular delivery, Ionic gelation.

Correspondence:
Dr. Divya Juyal
Professor and Dean, Department of Pharmacognosy, School of Pharmaceutical Sciences, Shri Guru Ram Rai University, Patel Nagar Campus, Patel Nagar, Dehradun, Uttarakhand-248001, INDIA.
Email: divya.jl@sgrru.ac.in

Received: 03-11-2025;
Revised: 28-12-2025;
Accepted: 12-02-2026.

INTRODUCTION

Herpes Simplex Virus (HSV)-induced eye disease is the most prevalent Infectious cause of unilateral corneal blindness and a major contributor to ocular morbidity in affluent nations.[1] The condition known as Herpes Simplex Virus (HSV) keratitis affects the transparent dome covering the colourful portion of the eye is called the cornea.[2] The most prevalent herpes virus associated with ocular infections is Herpes Simplex Type 1 (HSV-1). Although it can also infect ocular tissues, Herpes Simplex Type 2 (HSV-2) is most frequently observed in neonatal conditions.[3] Acute primary blepharokeratoconjunctivitis and chronic recurrent keratitis are the most common manifestations caused by HSV ocular infections.[4] Deeper infections can result in lesions defined by dendritic keratitis, whereas superficial infections typically leave no scarring.[5] An immune-mediated inflammatory process that typically results in blindness can produce scarring due to recurrent infections.[6]

DOI: 10.5530/ijper.20262668

The complicated structure and physiological barriers of the eye make it impossible for drug molecules to enter the site of action, making drug delivery to the ocular tissues challenging.[7] The first option for both the patient and the doctor, if there is any eye complication, is the conventional ophthalmic drug delivery method, such as eye drops.[8] Eye drops' main drawback is their low drug bioavailability due to some factors, including metabolic degradation, lachrymation and nasolachrymal drainage, which reduces the residence duration (less than 5 min) after administration.[9] Moreover, only 1-6% of the administered drug penetrates the intraocular space due to the cornea's relative impermeability.[10]

According to the US Pharmacopoeia and European Pharmacopoeia's solubility classification, GCV is "slightly soluble" (2 g/L). Furthermore, according to FDA recommendations, GCV was classified as having low permeability and categorised as Biopharmaceutics Classification System (BCS) Class 3 based on permeability studies.[11] GCV solubility is dependent on pH. With pKa values of 2.50 and 9.57, respectively, it is a weakly basic drug that dissolves in strong acids and bases. However, in the pH range of 4 to 8, it is either somewhat soluble or insoluble.[12]

The study aimed to formulate and optimize Ganciclovir-loaded chitosan nanoparticles for enhanced transcorneal permeation and sustained release of the dosage form to treat viral infection.

Moreover, the generated nanoparticles physicochemical characteristics were evaluated.

MATERIALS AND METHODS

Materials

The study used the following materials: Ganciclovir (Yarro Chem Ltd., Mumbai), and other chemicals, including chitosan, Sodium Tripolyphosphate (STPP), and acetic acid, were procured from Sisco Research Laboratories (SRL).

Methods

Preparation of chitosan-loaded nanoparticles

Chitosan (0.1%, 0.5% and 1%) and the required drug quantity were dissolved in 1% CH_3COOH solution and agitated for 2 hr. TPP was taken at different concentrations (0.1%, 1%, 2%) in 10 mL of distilled water and stirred for 2 hr. Add the TPP solution dropwise to the chitosan solution, stir it for 2 hr, and sonicate it for 5 min.[13]

Evaluation Parameters of Nanoparticles

FTIR

The FTIR spectra for Ganciclovir in its pure form were obtained using an FTIR (Thermo Scientific Nicolet Summit LITE iD1). FTIR analysis was conducted to evaluate the physical and chemical interaction of the drug with the excipients using the Potassium bromide disk method.[14]

DSC

The DSC thermograms of pure Ganciclovir and the Physical mixture of Ganciclovir, chitosan and STPP were obtained using the Thermal DSC analyzer (Perkin Elmer, Pyris-6, Jamia Hamdard). After being precisely weighed into an aluminium pan and covered with an aluminium cover, the sample was heated from 30.0°C to 300.0°C at a rate of 10°C per minute.[15]

Particle size and PDI

The dynamic light scattering method determined the PDI and average particle size of the nanoparticles. The two most important characteristics of nanocarriers that determine their physical stability are their particle size and Polydispersity Index (PDI).[16]

Zeta potential

Electrostatic repulsion can stabilize nanoformulations at high zeta potential values (>±30 mV). On the other hand, positively charged particles work better to increase electrostatic interaction with the eye's negatively charged surface. The zeta potential was identified by using the Malvern Instrument (zeta sizer ver. 7.11).[17]

Entrapment Efficiency and Drug Loading

Nanocarriers must transport a sizable drug payload to prevent drug waste during formulation. To evaluate the entrapment efficiency of a nanoformulation, the unentrapped and entrapped drugs are usually separated by centrifugation at 10,000-20,000 rpm for 10-30 min.[18]

In vitro drug release study

The dialysis membrane with a molecular weight cutoff of 12000-14000 kDa was used to study the *in vitro* release of ganciclovir from the formulation. Freshly made artificial tear fluid (pH 7.4) served as the diffusion medium. An accurately measured 2 mL volume of the formulation was precisely pipetted into a dialysis membrane that had been soaked in the diffusion medium overnight. The membrane was tied from both ends. At (37±0.5) °C, the dialysis membrane was suspended in a beaker filled with 100 mL of diffusion media. In this case, 100 mL was chosen with consideration for the sink condition, and the formulation was visible throughout the study. This assembly was maintained at 50 rpm on a magnetic stirrer. A UV-vis spectrophotometer (LABMAN LMSP-UV 1900) was used to analyze the aliquots at 250 nm after diluting them with dissolving buffer.[19]

Surface Morphology

Nanoparticles' surface shape influences their biodistribution, cellular uptake, and toxicity. Different shapes, such as spheres, cubes, and rods, can be seen in nanoparticles. Spherically shaped nanoparticles can achieve better drug performance.[20] Transmission Electron Microscopy (TEM) and Scanning Electron Microscopy (SEM) are commonly used to study the structure of nanoparticles. SEM depicts the particle's surface morphology and structure, while TEM shows the particle's internal structure, size, and shape. A TEM device (Thermo Scientific, TALOS L 12°C G2, Jamia Hamdard) was used to take the sample images. SEM analysis has been used to evaluate the particle's shape and surface characteristics. Double-sided tape was used to attach the nanoparticles to aluminium stubs.[21] A SEM device (ZEISS) was used to take the sample images.

RESULTS

Fourier Transform Infrared Spectroscopy

The FTIR spectrum was recorded to assess the purity of the drug ganciclovir. A potassium bromide pellet method was employed for the identification of the functional group of the drug by FTIR analysis. FTIR spectra of the drug ganciclovir were observed between scanning ranges of 400-4000 cm^{-1}. Ultimately, the reference spectra and the resultant spectrum were compared as shown in Figure 1A and the FTIR of the drug physical mixture is shown in Figure 1B. The characteristic peaks of each component with minor shifts and widening around 3400 cm^{-1} and 1600 cm^{-1} were visible in the FTIR spectra of the physical mixture of ganciclovir, chitosan, and sodium tripolyphosphate, suggesting hydrogen bonding and ionic interactions. When phosphate bands (1250-900 cm^{-1}) are present, it indicates that the drug is compatible and that there is no chemical degradation of the

Table 1:FTIR interpretation of Ganciclovir.

Sl. No.	Functional Group	Peak Characterization	Peak observed
1	C-N (aromatic)	1615-1700	1655.62
2	N-H	3300-3500 3100-3500	3418.54 3151
3	O-H (H- bonded)	3200-3600	3322.35
4	C-N (aliphatic)	1080-1360	1056
5	C=O	1640-1690	1655.62

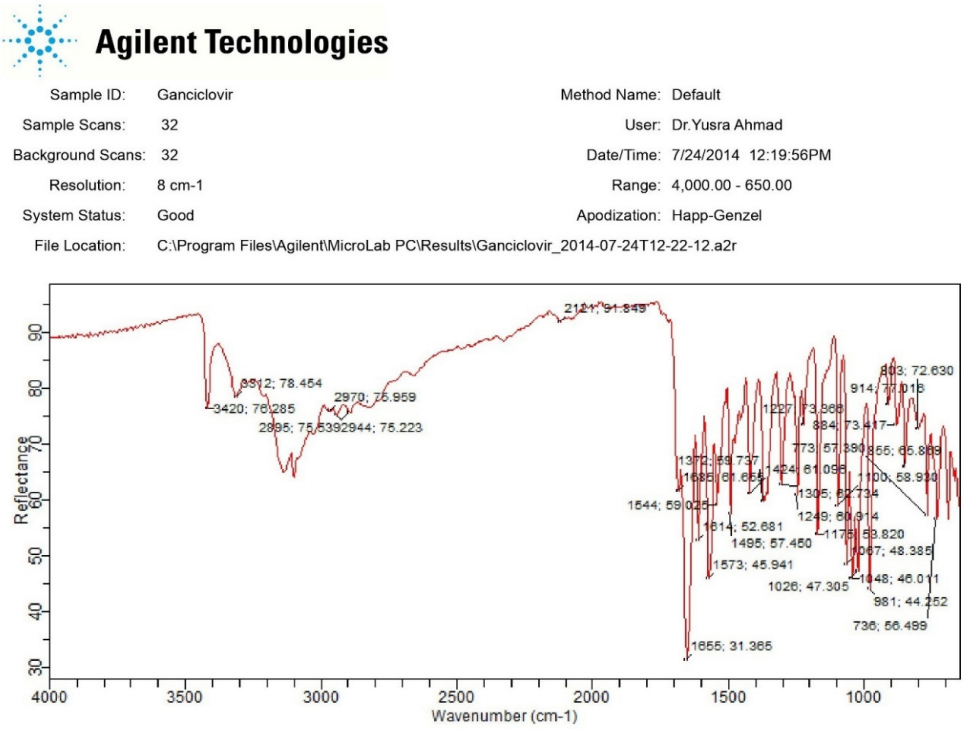

Figure 1A: FTIR spectra of pure drug Ganciclovir.

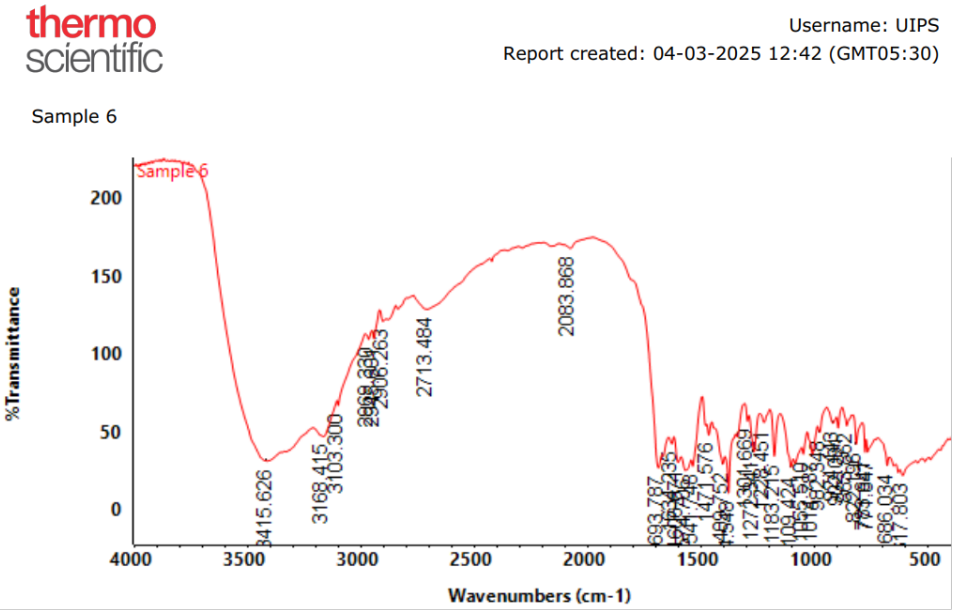

Figure 1B: FTIR spectra of the drug and physical mixture.

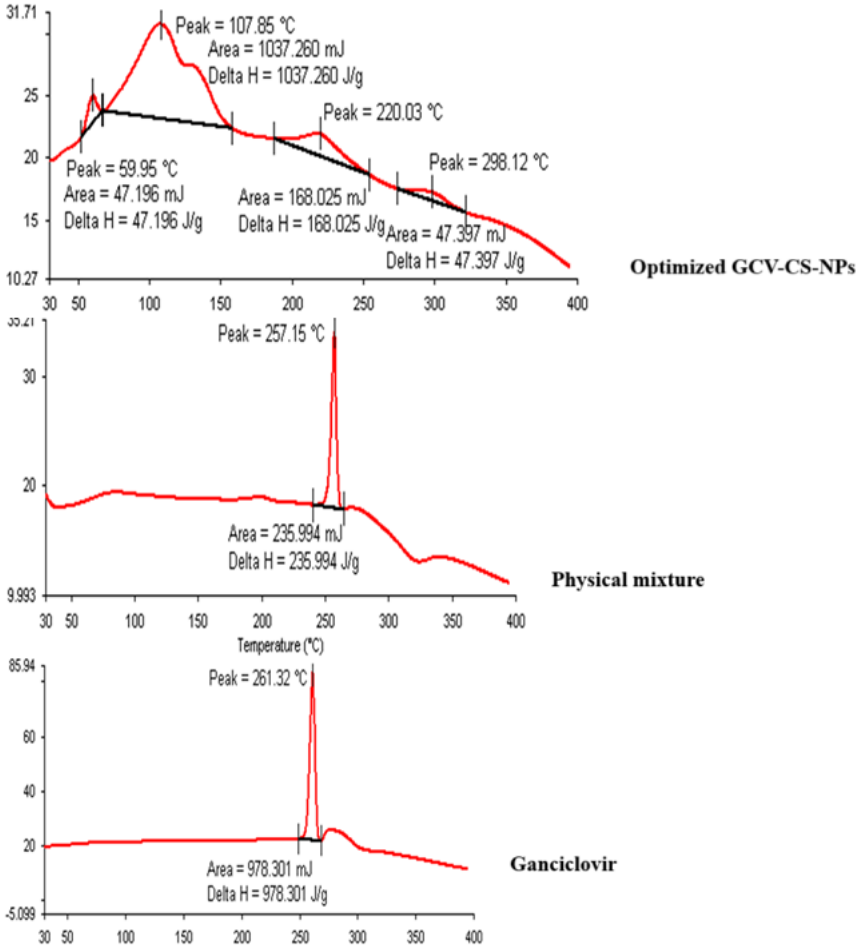

Figure 1C: DSC curve of Ganciclovir, physical mixture, and optimized GCV-CS-NPs.

chitosan-TPP crosslinking. The interpretation of the drug is given in Table 1.

Figure 1C shows the optimal GCV-CS-NPs, physical mixture, and GCV DSC thermogram. The crystalline character of GCV was shown by the prominent endothermic peak at 261.32°C in the DSC thermogram. Additionally, there were noticeable peaks of GCV at 257.15°C in the DSC thermogram of the physical mixing of the solid samples (GCV, STPP and CS) which shows the compatibility between the drug and excipients. Additionally, due to GCV's entrapment in the NPs matrix in an amorphous condition, the DSC thermogram of GCV-CS-NPs showed the peak of GCV. The melting point of GCV-CS-NPs showed numerous endothermic peaks at 59.5°C, 107.85°C, 220.03°C and 298.12°C, which shows that the formulation exhibits clear thermal transitions, which is common in nanoparticles because of component behaviour alteration and encapsulation.

DISCUSSION

Optimization data analysis, and experimental validation

The Box-Behnken design approach was used to optimise the prepared GCV-CS-NPs. The trial version of Design Expert Software (STAT-EASE360) was used to fit the responses of all fifteen formulations to various models and analyse the experimental results. Quadratic models were found to be the most appropriate for the tested parameters, which include entrapment efficiency, cumulative drug release, and drug loading. The 3D response surface plot and contour plot were used to evaluate the impact of independent variables on dependent variables.

To produce NPs, the independent variables CS (%, X1), TPP (%, X2), and Sonication time (mins, X3) have been taken at three different levels (low, medium, and high), as shown in Table 2. To prepare NPs, the concentration range was as follows: CS (X1) was 0.1% (low) to 1% (high), TPP (X2) was 0.1% (low) to 2% (high), and the sonication time was 1 min (low) and 10 min (high). To verify an error in the results of the same three compositions, the design showed 15 formulations with three centre points. The drug encapsulation efficiency (Y1) was found in the range of

Table 2:Observed GCV-CS-NPS Box-Behnken experimental runs with their actual and expected experimental values for drug loading (Y3), cumulative drug release (Y2), and encapsulation efficiency (Y1).

Runs	Independent variable			Dependent Variables					
	X1	X2	X3	Y1		Y2		Y3	
				Actual	Predicted	Actual	Predicted	Actual	Predicted
F1	0.55	2	10	92.36	93.06	94.42	94.89	17	18
F2	0.55	2	1	76.02	75.89	91.64	92.21	16	16
F3	0.1	1.05	10	94.09	94.02	87.73	87.16	18	18
F4	0.55	1.05	5.5	84.17	85.31	92.51	92.93	15	16
F5	1	1.05	10	93.13	93.25	90.07	91.11	17	17
F6	0.55	1.05	5.5	85.12	86.57	93.36	93.67	13	14
F7	1	1.05	1	77.13	77.44	92.88	92.24	16	16
F8	1	2	5.5	86.32	86.26	89.65	89.91	14	15
F9	0.55	1.05	5.5	86.16	87.10	94.38	95.18	14	14
F10	0.1	0.1	5.5	85.16	85.22	88.04	88.75	13	13
F11	0.55	0.1	10	91.07	92.78	94.21	94.79	18	18
F12	0.55	0.1	1	75.09	76.31	95.96	95.43	15	16
F13	0.1	1.05	1	75.06	75.49	87.78	88.13	15	15
F14	0.1	2	5.5	87.15	87.65	86.57	86.80	13	13
F15	1	0.1	5.5	86.17	86.54	91.82	91.16	14	14

X1= Concentration of Chitosan (%), X2= Concentration of TPP (%), X3= Sonication time (mins), Y1= Encapsulation efficiency (%), Y2= Cumulative drug release (%), Y3= Drug loading (%).

Table 3:Summary of regression analysis and analysis of variance for response I (Entrapment Efficiency), response II (Drug release) and response III (Drug loading).

Parameters	DF	SS	MS	F	*p*-value	R^2	SD	CV	Outcome
Entrapment efficiency									
Model	9	586.09	65.12	108.23	0.0276	0.9949	84.95	91.31	Significant
Residual	5	3.01	0.6017						
Total	14	589.1	65.7217						
Drug Loading									
Model	9	39.90	4.43	8.87	0.0135	0.9410	15.20	4.65	Significant
Residual	5	2.50	0.5000						
Total	14	42.4	4.93						
Drug Release									
Model	9	116.50	12.94	17.42	0.0029	0.9691	91.40	94.30	Significant
Residual	5	3.71	0.7429						
Total	14	120.21	13.6829						

75.06% (F12) to 90.04% (F3). The drug release (Y2) was found in the range of 86.57% (F14) to 95.96% (F12), and the drug loading was found in the range of 13% (F11) to 18% (F14). As shown in Table 2, the practical value result was extremely close to the actual value. The linear correlation between the actual and predicted values was shown in Figure 2a. The software ran an Analysis of Variance (ANOVA) to each response, and the results show that the model suited the data well (Table 3).

Impact of independent variables on the entrapment efficiency

Figure 2b shows the response graph (3D plot and contour plot) that illustrates the impact of independent factors. It showed that the impact of each factor on %EE was well-defined. The

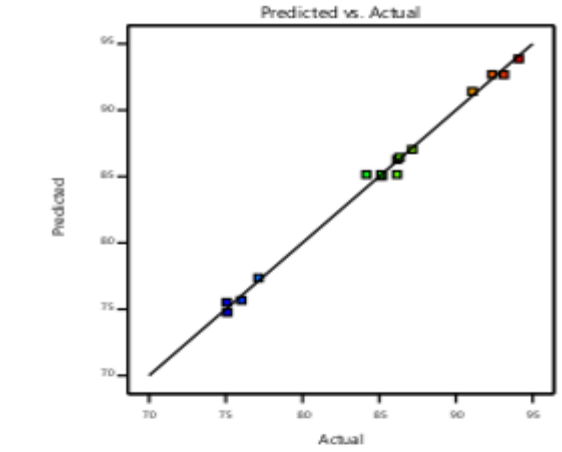

a)

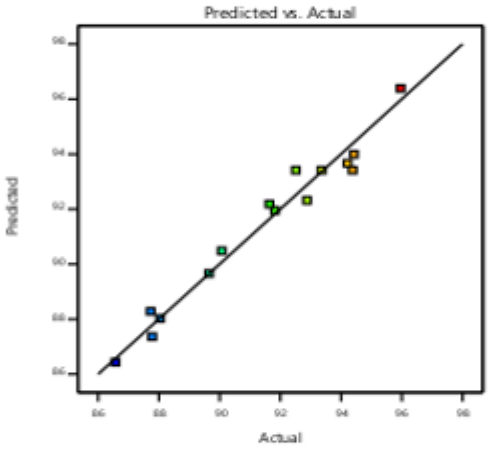

b)

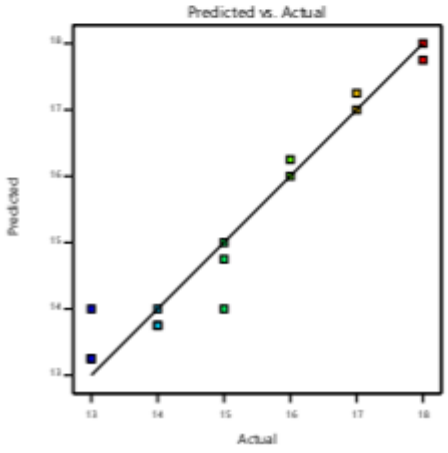

c)

Figure 2A: Linear correlation between the Actual and Predicted value of A (encapsulation), B (Drug loading) and C (Drug release).

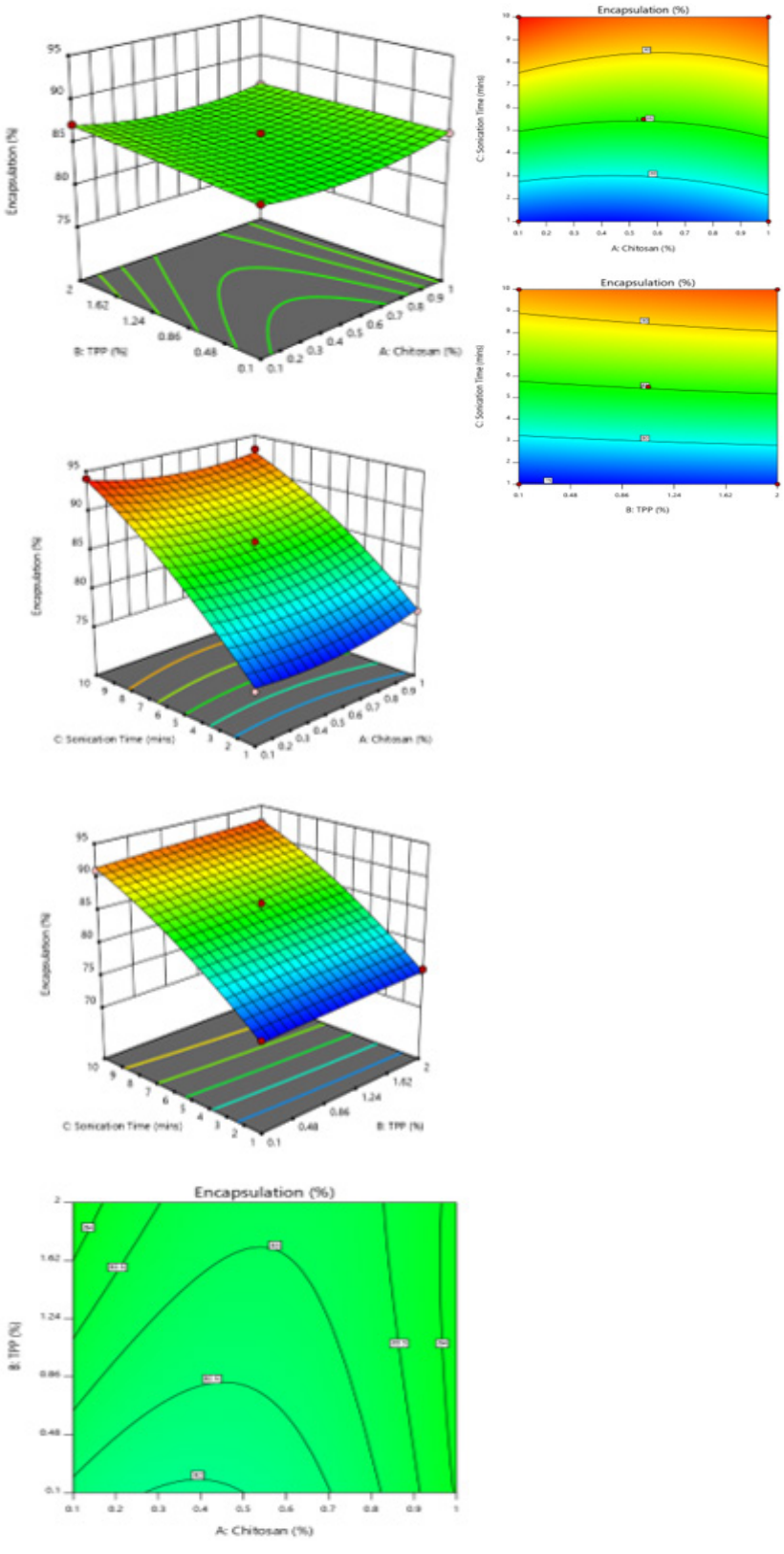

Figure 2B: The impact of independent variables (X1 = chitosan; X2 = TPP; X3 = sonication duration) on encapsulation efficiency for GCV-CS-NPS is depicted in this 3D and contour response surface plot image.

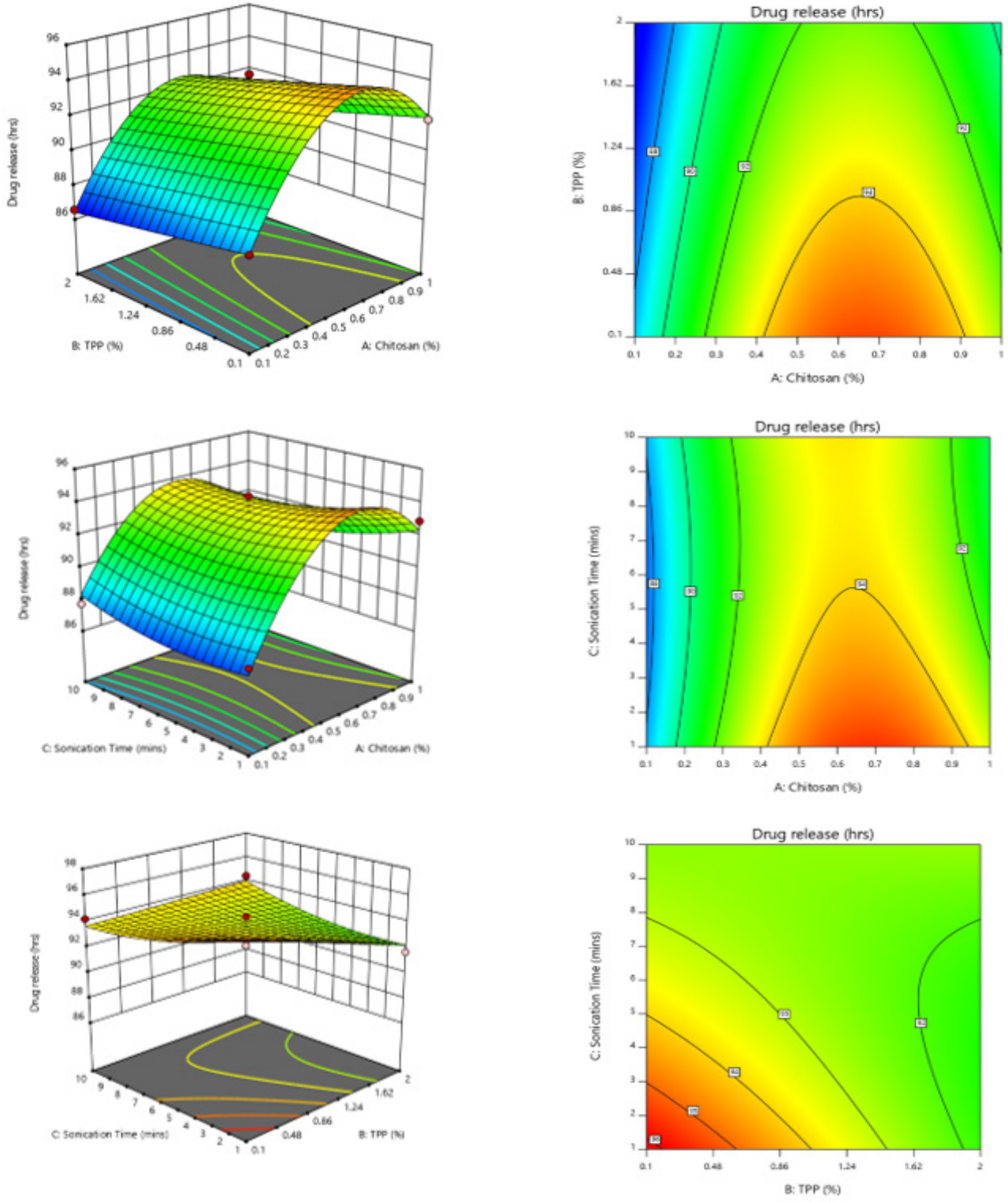

Figure 2C: The impact of independent factors (X1 = chitosan; X2 = TPP; X3 = sonication duration) that affect cumulative drug release for GCV-CS-NPS are depicted in this three-dimensional and contour response surface plot image.

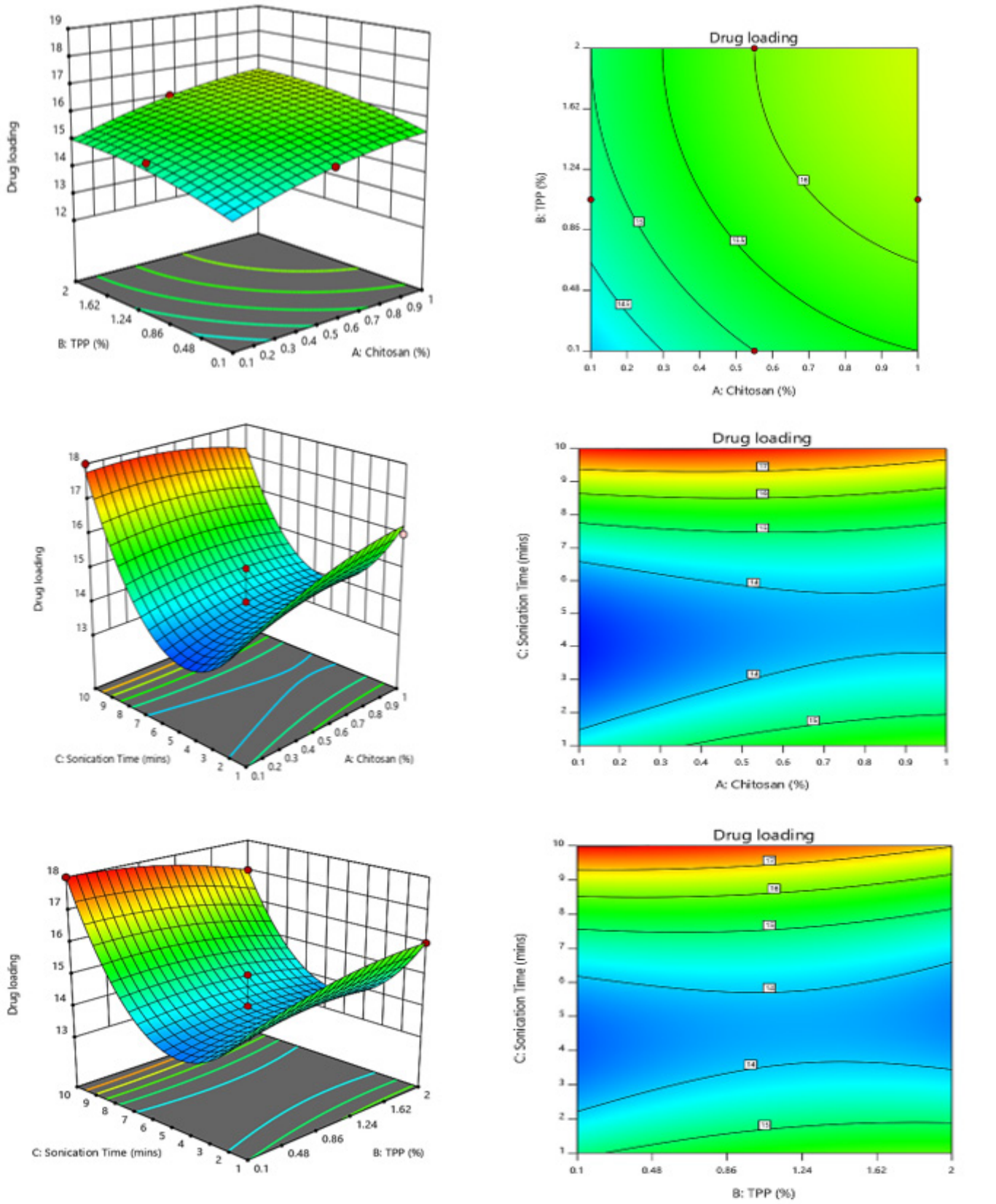

Figure 2D: Impact of drug loading for GCV-CS-NPS as influenced by independent factors (X1 = PCL; X2 = CS; X3 = PVA) in a 3-D and contour response surface plot image.

polynomial equation showed that the variables A (chitosan), B (TPP) and C (Sonication time) have a positive effect on the encapsulation (p<0.0001). The model F value of 108.23 implies that the model is significant. The model's best fit and reliability are shown by the lower p-value and greater F-value. Individually and in combination, each of these factors has demonstrated significant effects on %EE. Figure 2a shows that the actual and predicted R2 values matched closely, indicating that the model is credible in choosing the most reliable formulation.

Entrapment efficiency (Y1) = +85.15+0.1612A+0.5450B+8.42C-0.4600AB-0.7575AC+0.0900BC+1.13A2-0.0873B2-1.43C2.

Effect of the independent variable on cumulative drug release

Due to the higher available surface area, the smaller particle releases the drug more rapidly and effectively. The burst release behaviour arises from the smaller particles. Larger NPs have a slower drug release pattern because they have less surface area available for diffusion and penetration. Figure 2c shows the response graph (3D plot and contour plot) that illustrates the impact of independent factors. As the concentration of polymer (X1) increases, the release of GCV from GCV-CS-NPs increases and when the concentration of polymer (X2) increases, the release of drug from the NPs decreases. The variable (X3), sonication time has a positive impact on drug release.

Cumulative drug release (Y2) = 93.4167 + 1.7875A -0.96875B -0.22875C -0.175 AB -0.69 AC + 1.1325BC -4.41958 A2 + 0.0229167 B2 + 0.617917C2

The polynomial equation indicated that the variable CS (X1) had a positive effect on drug release, while TPP (X2) had a negative impact (p<0.0001). Drug release has been positively impacted by the third variable, sonication time (X3) (p<0.0001). Additionally, the combination of TPP (X2) and Sonication time (X3) had positive effects on drug release. The significance of the model is indicated by its F-value of 17.42. Individually and in combination, each of these factors has demonstrated significant effects on cumulative drug release. Figure 2a shows that the actual and predicted R2 values matched closely, indicating that the model is credible in choosing the most reliable formulation.

Effect of the independent variable on Drug loading

Figure 2d shows the response graph (3D plot and contour plot) that illustrates the impact of independent factors. It showed that the impact of each factor on %drug loading was well-defined. Drug loading was positively impacted by the factors CS (X1), TPP (X2), and sonication duration (X3), according to the polynomial equation. While the combined impact of variable CS: Sonication time and variable TPP: Sonication time had a detrimental effect on drug loading, the combination effect of variables CS and TPP also shown a beneficial effect.

% Drug loading (Y3) = 14.00+0.2500A+0.1568B+1.26C+4.632AB-0.523AC-0.587BC-0.25A2-0.284B2+2.75C2

The model F value of 19.60 implies that the model is significant. The lower p-value and greater F-value show the model's best fit and reliability. Individually and in combination, each of these factors has demonstrated significant effects on % drug loading. Figure 2a shows that the actual and predicted R2 values matched closely, indicating that the model is credible in choosing the most reliable formulation.

Selection of optimized GCV-CS-NPs

Using Design Expert® software, the highest entrapment efficiency, cumulative drug release, and drug loading criteria were used to optimise the GCV-CS-NPs, with chitosan (1%), TPP (0.1%), and sonication time (5 min) found to meet the requirements for an optimized nanoparticle. Predicted values were R1 = 95.05%, R2 = 93.43%, and R3 = 18.31%. The optimized GCV-CS-NPs exhibited, %EE of 92.17%, a cumulative drug release of 90.82 %, and a drug loading of 17%, respectively.

Particle size and Polydispersity Index (PDI)

The particle size and PDI of all 15 formulations range from 120 nm to 419 nm and 0.23 to 0.68. The PDI of the optimized formulation is found to be 0.223 and size 120 nm, which is good for the ocular delivery as shown in Figure 3a.

Zeta Potential

The zeta potential of all 15 formulations ranges from -24 mV to -20 mV as shown in Figure 3b. The zeta potential of the optimized formulation is found to be -20 mV. It is generally acknowledged that a significant magnitude (positive or negative) of the zeta potential, i.e., larger than or equal to +30 mV or -30 mV, signifies the electrostatic stability of the particle suspension.

Entrapment Efficiency and Drug Loading

All 15 nanoformulations had entrapment efficiencies ranging from 70.05 to 94.22. The optimized formulation, which has a low concentration of the cross-linking agent, has an entrapment efficiency of 92.17%.

In vitro drug release study

According to the *in vitro* drug release data, Figure 4 illustrates the sustained release percentage from the generated nanoparticle formulations F1-F15, which ranges from 83.57% to 95.96% for up to 12 hr. The *in vitro* drug release of the optimized formulation is shown in Table 4. Even after 12 hr, 10% of the drug remains in the nanoparticles, showing that the release is sustained.

Kinetic modelling and drug release mechanism

The drug release data were evaluated using the Hixon-Crowell, Higuchi, Korsemeyer Peppa's, first-order, and zero-order kinetics following the fitting of the dissolution profiles to several models, as

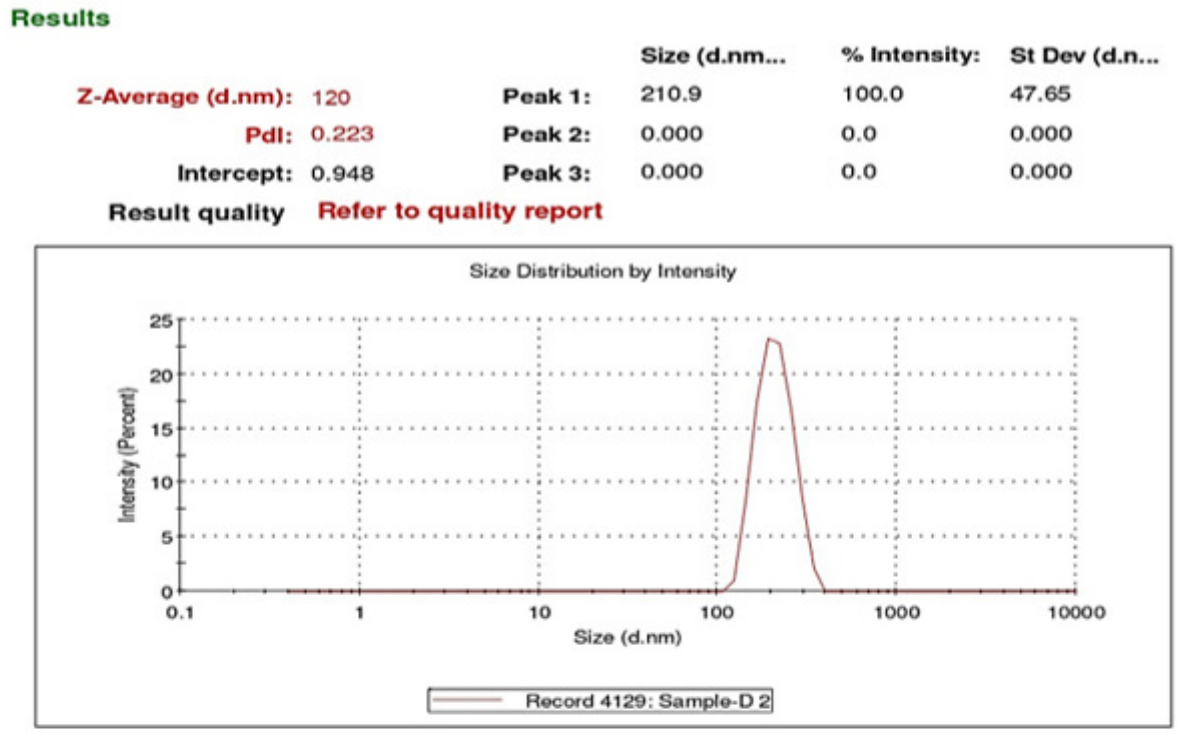

a)

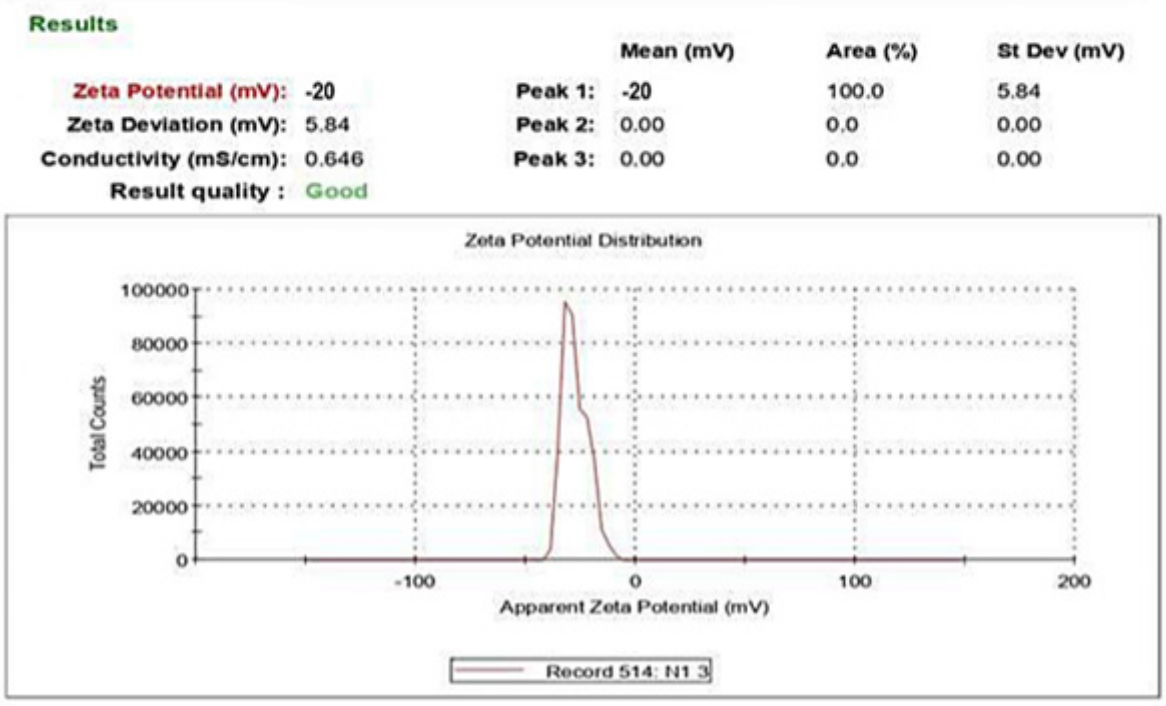

b)

Figure 3: (a) PDI image of the optimized formulation, (b) Zeta potential image of the optimized formulation.

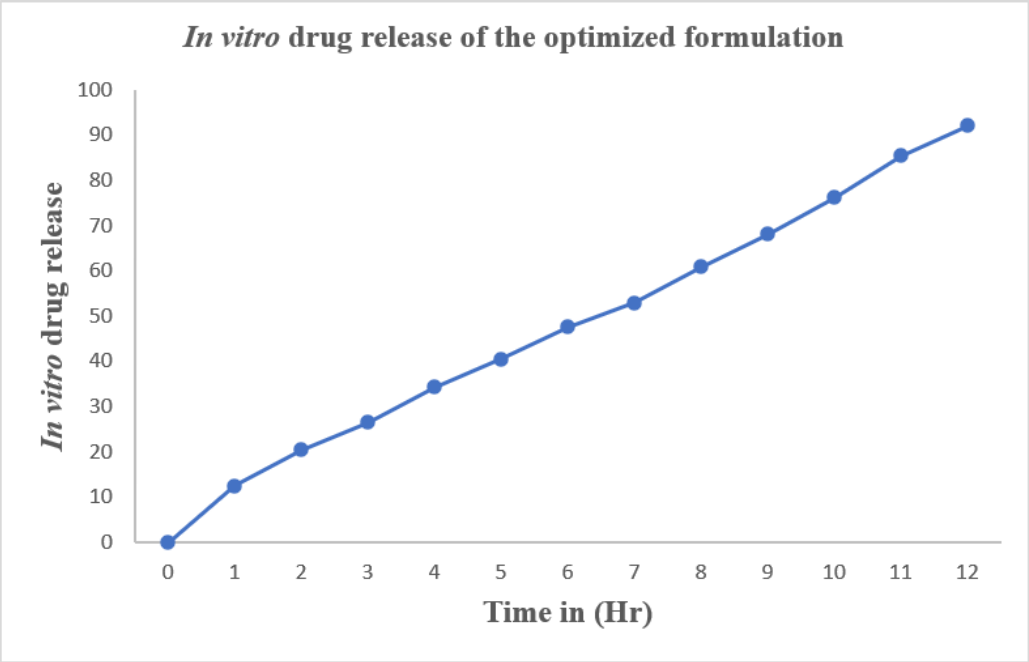

Figure 4: *In vitro* drug release of the optimized formulation.

Table 4: ***In vitro*** **drug release of the optimized formulation.**

Time (hr)	% drug release
1	12.43
2	20.46
3	26.46
4	34.27
5	40.45
6	47.54
7	52.88
8	60.81
9	68.09
10	76.16
11	85.37
12	92.04

Table 5:Kinetic Modelling of the optimized formulation.

Models	R^2	R^2 observed	SSR	MSC
Zero-order	0.9918	0.9983	19.6276	4.3845
First-order	0.9494	0.9794	493.670	2.5673
Higuchi	0.8940	0.9671	1034.3140	1.8276
Korsmeyer- Peppas	0.9963	0.9980	35.7585	5.6360
Hixson-Crowell	0.9730	0.9879	263.8352	3.1937

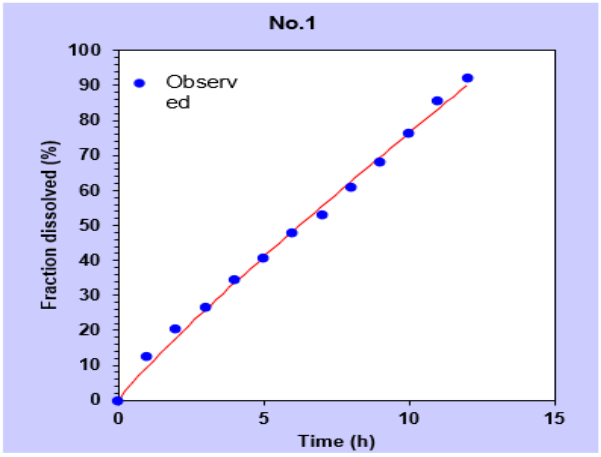

a)

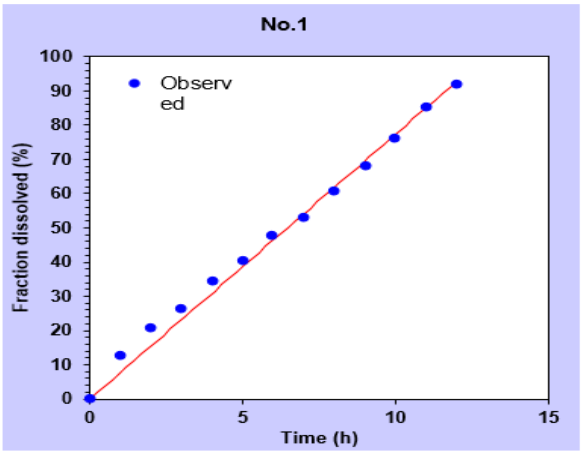

b)

Figure 5: Graph obtained from the Drug release kinetics of optimized formulation (A), Korsemeyer Peppas and (B) zero order.

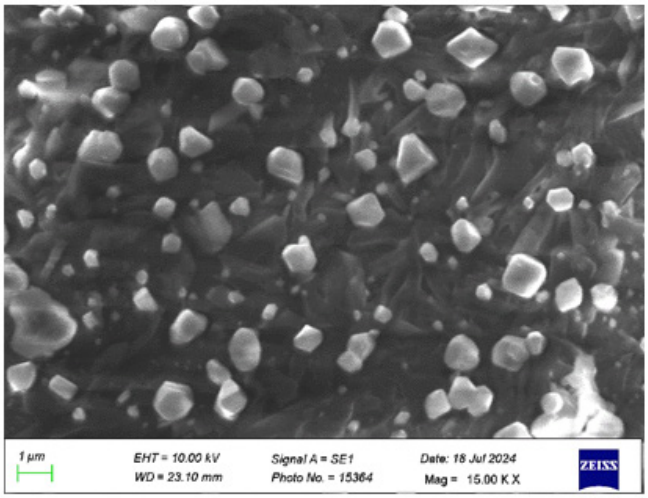

a)

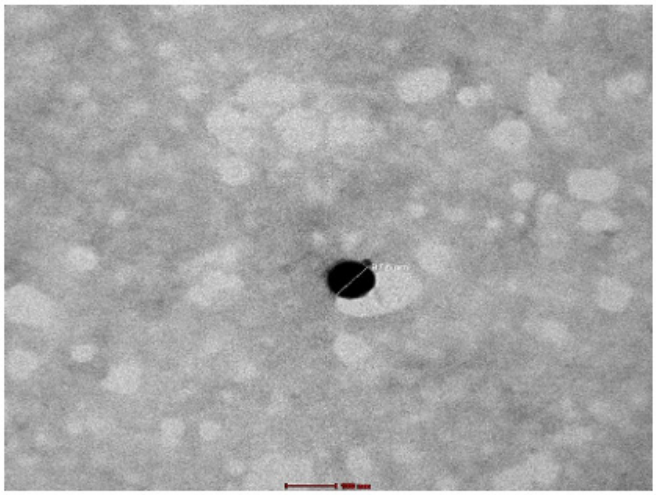

b)

Figure 6: (a) SEM images of the optimized formulation, (b) TEM images of the optimized nanoparticles.

demonstrated in Table 5. The drug release from the nanoparticles was best explained by zero-order and Korsmeyer Peppa's model, (Figure 5) as shown by the good linearity of R^2 and the n value above 0.5 and 1 in Table 5 shows the transport mechanism is a non-Fickian diffusion mechanism involving both drug diffusion and polymer erosion.

SEM

SEM was used to analyze the surface morphology of the dried optimized nanoparticle formulation, as seen in Figure 6a. It was discovered that every particle was round and smooth, which is favourable for ocular delivery.

TEM

TEM was used to evaluate the nanoparticles' morphology. The size and structure of the nanoparticles are revealed by TEM. As seen in Figure 6b, the prepared nanoparticles were found to be spherical.

CONCLUSION

The GCV-CS-NPs were successfully developed by the ionic gelation method. To optimize the formulation parameters, BBD was utilized to assess the interaction and quadratic impacts of the three primary influencing factors that were selected: entrapment efficiency, cumulative drug release, and drug loading. The optimize formulation for the nanoparticles was found to be 1% chitosan, 0.1% TPP, and 5 min of sonication time based on the experimental results and a mathematical evaluation of the constraints. The optimized formulation showed particle size of 120 nm and PDI of 0.223, Zeta potential of -20 mV, Entrapment efficiency of 91.93, *in vitro* drug release of 92.27% up to 12 hr in simulated tear fluid, Drug loading of 17.68% Transmission electron microscopy verified its excellent dispersibility and cubic form. All these results demonstrate that the optimised formulation of GCV-CS-NPs is ideal for ocular delivery, as it increases its therapeutic efficiency by improving eye penetration and prolonging ocular retention time. It offers superior patient compliance and efficacy over conventional eye drops due to its sustained release and prolonged retention period.

ACKNOWLEDGEMENT

The authors would like to express their gratitude to the authorities of the School of Pharmaceutical Sciences, Shri Guru Ram Rai University, Dehradun, for providing the necessary laboratory facilities for this project.

ABBREVIATIONS

GCV: Ganciclovir, **CS:** Chitosan, **STTP:** Sodium Tripolyphosphate, **PDI:** poly dispersity index, **NPs:** nanoparticles, **BBD:** Box Behnken design, **SEM:** Scanning electron microscopy, **TEM:** Transmission electron microscopy, **GCV-CS-NPs:** Ganciclovir loaded Chitosan Nanoparticles.

CONFLICT OF INTEREST

The authors declare that there is no conflict of interest.

SUMMARY

The study aimed to optimize Ganciclovir-loaded nanoparticles for ocular delivery by evaluating the relationship between experimental data and Design factors. A three-level, three-factor Box-Behnken Design (BBD) was used for the optimisation process. Selecting the concentrations of chitosan, Sodium Tripolyphosphate (STPP) and sonication time as the independent

variables. Nanoparticles were prepared by using the ionic gelation method. The prepared ganciclovir-loaded chitosan nanoparticles showed an entrapment efficiency of 91.93%, a Cumulative drug release of 92.27% and % drug loading of 17.68. Biphasic behaviour was demonstrated by the GCV release from GCV-CS-NPS, which burst for 2 hr after a 12-hr sustained release, followed by zero order and Korsmeyer-Peppas model.

REFERENCES

1. Chou TY, Hong BY. Ganciclovir ophthalmic gel 0.15% for the treatment of acute herpetic keratitis: Background, effectiveness, tolerability, safety, and future applications. Ther Clin Risk Manag 2014;10(1):665-81.
2. Ivanina A, Leneva I, Falynskova I, *et al.* The Topical Novel Formulations of Interferon α-2в Effectively Inhibit HSV-1 Keratitis in the Rabbit Eye Model and HSV-2 Genital Herpes in Mice. Viruses 2024; 16: 989 [homepage on the Internet] 2024 [cited 2025 May 1];16(6):989. Available from: https://www.mdpi.com/1999-4915/16/6/989/htm
3. Sheng Q, Zhai R, Fan X, Kong X. 2% Ganciclovir Eye Drops Control Posner-Schlossman Syndrome Relapses With/Without Cytomegalovirus Intraocular Reactivation. Front Med (Lausanne) 2022;9:848820.
4. Shen W, Wang C, Jiang J, He Y, Liang Q, Hu K. Targeted delivery of herpes simplex virus glycoprotein D to CD169+ macrophages using ganglioside liposomes alleviates herpes simplex keratitis in mice. Journal of Controlled Release [homepage on the Internet] 2024 [cited 2025 May 1];365:208-18. Available from: https://www.sciencedirect.com/science/article/abs/pii/S0168365923007435
5. Domenech-Monsell IM, Alambiaga-Caravaca AM, Bernat-Just L, *et al.* Innovative Famciclovir Eye Drop Formulations for Herpes Zoster Infections. Curr Eye Res [homepage on the Internet] 2025 [cited 2025 May 1]; 1-10. Available from: http://www.ncbi.nlm.nih.gov/pubmed/40025627
6. Tian B, Bilsbury E, Doherty S, *et al.* Ocular Drug Delivery: Advancements and Innovations. Pharmaceutics 2022,Vol 14 Page 1931 [homepage on the Internet] 2022 [cited 2025 May 1]; 14(9): 1931. Available from: https://www.mdpi.com/1999-4923/14/9/1931/htm
7. Mahor A, Prajapati SK, Verma A, Gupta R, Iyer AK, Kesharwani P. Moxifloxacin loaded gelatin nanoparticles for ocular delivery: Formulation and *in vitro*, *in vivo* evaluation. J Colloid Interface Sci 2016;483: 132-8.
8. Chen Y, Kalia YN. Short-duration ocular iontophoresis of ionizable aciclovir prodrugs: A new approach to treat herpes simplex infections in the anterior and posterior segments of the eye. Int J Pharm [homepage on the Internet] 2018 [cited 2025 May 1];536(1): 292-300. Available from: https://www.sciencedirect.com/science/article/abs/pii/S0378517317311249
9. Ameeduzzafar, Imam SS, Abbas Bukhari SN, Ahmad J, Ali A. Formulation and optimization of levofloxacin loaded chitosan nanoparticle for ocular delivery: *In vitro* characterization, ocular tolerance and antibacterial activity. Int J Biol Macromol 2018;108:650-659.
10. Khiev D, Mohamed ZA, Vichare R, *et al.* Emerging Nano-Formulations and Nanomedicines Applications for Ocular Drug Delivery. Nanomaterials 2021, Vol 11 Page 173 [homepage on the Internet] 2021 [cited 2024 Nov 9]; 11(1): 173. Available from: https://www.mdpi.com/2079-4991/11/1/173/htm
11. Suriyaamporn P, Pornpitchanarong C, Pamornpathomkul B, *et al.* Ganciclovir nanosuspension-loaded detachable microneedles patch for enhanced drug delivery to posterior eye segment. J Drug Deliv Sci Technol 2023;88: 104975.
12. Shah S, Patel V. Targeting posterior eye infections with colloidal carriers: The case of Ganciclovir. Int J Pharm 2023;645:123427.
13. Kalam MA. Development of chitosan nanoparticles coated with hyaluronic acid for topical ocular delivery of dexamethasone. Int J Biol Macromol 2016; 89: 127-136.
14. Pillai AR, Prajapati B, Dharamsi A. Protein Nanoparticles Laden *in situ* Gel for Topical Ocular Drug Delivery. Curr Drug Deliv [homepage on the Internet] 2023 [cited 2024 Jun 17];21(1): 38-51. Available from: https://benthamscience.com/article/129019
15. Shivam U U, Siddhi K C, Devarshi U G, Umeshkumar M U, Jayvadan K P. Nanoparticles laden *in situ* gel for sustained drug release after topical ocular administration. J Drug Deliv Sci Technol 2020;57:101736.
16. Singh M, Guzman-Aranguez A, Hussain A, Srinivas CS, Kaur IP. Solid Lipid Nanoparticles for Ocular Delivery of Isoniazid: Evaluation, Proof of Concept and *in vivo* Safety and Kinetics. Nanomedicine [homepage on the Internet] 2019 [cited 2025 May 1]; 14(4): 465-491. Available from: https://www.tandfonline.com/doi/abs/10.2217/nnm-2018-0278
17. Kalam MA, Iqbal M, Alshememry A, Alkholief M, Alshamsan A. Development and Evaluation of Chitosan Nanoparticles for Ocular Delivery of Tedizolid Phosphate. Molecules 2022,Vol 27 Page 2326 [homepage on the Internet] 2022 [cited 2025 May 1]; 27(7):2326. Available from: https://www.mdpi.com/1420-3049/27/7/2326/htm
18. Ameeduzzafar, Imam SS, Abbas Bukhari SN, Ahmad J, Ali A. Formulation and optimization of levofloxacin loaded chitosan nanoparticle for ocular delivery: *In vitro* characterization, ocular tolerance and antibacterial activity. Int J Biol Macromol [homepage on the Internet] 2018 [cited 2025 May 1]; 108: 650-659. Available from: https://www.sciencedirect.com/science/article/abs/pii/S0141813017315222
19. Laddha UD, Kshirsagar SJ. Formulation of nanoparticles loaded *in situ* gel for treatment of dry eye disease: *In vitro*, *ex vivo* and *in vivo* evidences. J Drug Deliv Sci Technol 2021;61:102112.
20. Eid HM, Elkomy MH, Menshawe SF El, Salem HF. Development, Optimization, and *in vitro/in vivo* Characterization of Enhanced Lipid Nanoparticles for Ocular Delivery of Ofloxacin: the Influence of Pegylation and Chitosan Coating. AAPS PharmSciTech [homepage on the Internet] 2019 [cited 2025 May 1]; 20(5): 1-14. Available from: https://link.springer.com/article/10.1208/s12249-019-1371-6
21. Suri R, Beg S, Kohli K. Target strategies for drug delivery bypassing ocular barriers. J Drug Deliv Sci Technol [homepage on the Internet] 2020 [cited 2025 May 1];55: 101389. Available from: https://www.sciencedirect.com/science/article/abs/pii/S1773224719314984?via%3Dihub

Cite this article: Verma S, Juyal D. Optimization of Ganciclovir-Loaded Nanoparticles for Ocular Delivery by Utilizing Box-Behnken Design. Indian J of Pharmaceutical Education and Research. 2026;60(2s):s826-s838.